

Research Article

Exploring the Potential Mechanisms of *Melilotus officinalis* (L.) Pall. in Chronic Muscle Repair Patterns Using Single Cell Receptor-Ligand Marker Analysis and Molecular Dynamics Simulations

Yisheng Chen,¹ Zhiwen Luo,¹ Jinrong Lin,¹ Beijie Qi,¹ Yaying Sun,¹ Fangqi Li,¹ Chenyang Guo,² Weiwei Lin,³ Xueran Kang,⁴ Xinyi He,⁵ Qian Wang ,⁶ Shiyi Chen ,¹ and Jiwu Chen ²

¹Department of Sports Medicine, Huashan Hospital, Fudan University, Shanghai, China

²Department of Orthopedics, Shanghai General Hospital, Shanghai Jiao Tong University School of Medicine, Shanghai Jiao Tong University, Shanghai 200080, China

³Department of Neurosurgery, Second Affiliated Hospital of Zhejiang University School of Medicine, Zhejiang University, 88 Jiefang Road, Hangzhou, 310009 Zhejiang, China

⁴Shanghai Jiao Tong University, Shanghai 200080, China

⁵State Key Laboratory of Genetics Engineering, Collaborative Innovation Center for Genetics and Development, School Life Sciences and Human Phenome Institute, Fudan University, Shanghai, China

⁶Postdoctoral Workstation, Department of Central Laboratory, The Affiliated Taian City Central Hospital of Qingdao University, Taian 271000, China

Correspondence should be addressed to Qian Wang; qianqianwangxi@163.com, Shiyi Chen; cshiyi@163.com, and Jiwu Chen; jeevechen@gmail.com

Received 17 December 2021; Revised 28 February 2022; Accepted 26 April 2022; Published 1 June 2022

Academic Editor: Alexander Berezin

Copyright © 2022 Yisheng Chen et al. This is an open access article distributed under the Creative Commons Attribution License, which permits unrestricted use, distribution, and reproduction in any medium, provided the original work is properly cited.

Information regarding the function of *Melilotus officinalis* (L.) Pall. in skeletal muscles is still unknown. In this study, we explored the possible regulatory targets of *M. (L.) Pall.* that affects the repair patterns in chronic muscle injury. We analyzed the potential target genes and chemical composition of *M. (L.) Pall.* and constructed a “drug-component-disease target genes” network analysis. Five active ingredients and 87 corresponding targets were obtained. Muscle-tendon junction (MTJ) cells were used to perform receptor-ligand marker analysis using the CellphoneDB algorithm. Targets of *M. (L.) Pall.* were screened further for the cellular ligand-receptor protein action on MTJs. Enrichment analysis suggests that those protein-associated ligand receptors may be associated with a range of intercellular signaling pathways. Molecular docking validation was then performed. Five proteins (CCL2, VEGFA, MMP2, MET, and EGFR) may be regulated by the active ingredient luteolin and scoparone. Finally, molecular dynamics simulations revealed that luteolin can stably target binding to MMP2. *M. (L.) Pall.* influences skeletal muscle repair patterns by affecting the fibroblast interactions in the muscle-tendon junctions through the active ingredients luteolin and scoparone.

1. Introduction

Melilotus officinalis (L.) Pall. (*M. (L.) Pall.*) is a traditional Chinese medicine that is widely distributed and has broad prospects for development and utilization [1]. *M. (L.) Pall.* has antiedema, antioxidant, and hepatoprotective properties

[1–3]. In ancient China, *M. (L.) Pall.* was used to treat a variety of chronic diseases [4]. *M. (L.) Pall.* is often used to reduce postoperative edema and promote early recovery after clinical orthopedic and sports medicine procedures. However, the function of *M. (L.) Pall.* in chronic skeletal muscle injury is unproven.

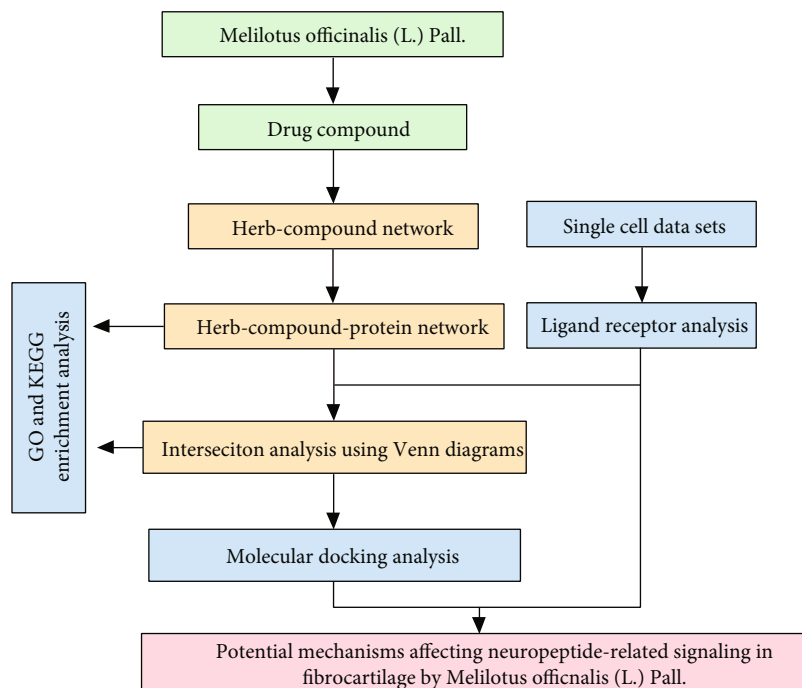


FIGURE 1: Research flow chart.

Skeletal muscle injuries are one of the most common sports injuries, accounting for approximately 40% of sports-related injuries in older people [5]. Muscles can be damaged by external forces, biological factors, and chemical factors [6, 7]. Excessive chronic injuries will lead to scar formation and fat infiltration [8, 9]. Therefore, understanding the factors influencing muscle repair can help promote skeletal muscle repair [10, 11]. Recent topical studies have explored the spatial-positional interactions of skeletal muscle regeneration and their underlying mechanisms to find new ways to improve the repair potential of skeletal muscles [12, 13]. Recent studies have found that the positional information driving limb muscle patterns are contained in the fibroblasts of the connective tissues [14]. Our previous studies have annotated and functionally analyzed these cells [15]. These cells have extensive intercellular interactions via the ligand-receptor pathway.

Liu et al. isolated 29 compounds from *M. (L.) Pall.* alcoholic extracts. They have good antioxidant activity and play an important role in anti-inflammatory and antioxidant functions [16]. Recent studies have also found that *M. (L.) Pall.* promotes wound repair [17]. This study provides a new way to explore these effects of *M. (L.) Pall.* in skeletal muscles by targeting the ligand-receptor pathway, which is important for drug function [18, 19]. Studying the effects of *M. (L.) Pall.* in the skeletal muscle fibroblasts allows us to explore its potential mechanisms in muscle repair patterns.

In this study, network pharmacology and molecular docking approaches have been used to predict the possible regulatory targets of *M. (L.) Pall.* in muscle repair patterns, to reveal the potential molecular mechanisms of this compound in regulating muscle repair patterns and provide new ideas for the treatment of skeletal muscle injury.

TABLE 1: Six active ingredients of *M. (L.) Pall.* were screened.

Molecule name	Molecule ID	OD	Drug-likeness
Scoparone	MOL001999	74.75	0.09
Ferulic acid	MOL000360	39.56	0.06
Soyasapogenol E	MOL003651	37.64	0.75
Beta-sitosterol	MOL000358	36.91	0.75
Luteolin	MOL000006	36.16	0.25
Salicylic acid	MOL001801	32.13	0.03

2. Materials and Methods

2.1. Screening for Active Ingredients and Targets of *M. (L.) Pall.* The active ingredients of *M. (L.) Pall.* were obtained from previous research results [16]. The active ingredients of *M. (L.) Pall.* were screened from the Traditional Chinese Medicine Systems Pharmacology Database and Analysis Platform (TCMSP) [20] database using the following conditions: oral bioavailability (OB) $\geq 30\%$ and drug-likeness (DL) ≥ 0.1820 . Potential target genes of *M. (L.) Pall.* were obtained by converting the screened active ingredients into corresponding targets through the UniProt database (<http://www.uniprot.org/>).

2.2. “Drug-Component-Target” Network Construction. A “drug-component-target” network structure was constructed with the active ingredient and corresponding target genes of *M. (L.) Pall.* using the Cytoscape (version 3.7.2) software [21]. Each node and edge in the network was analyzed to determine the relationship between the diseases and drug actions.

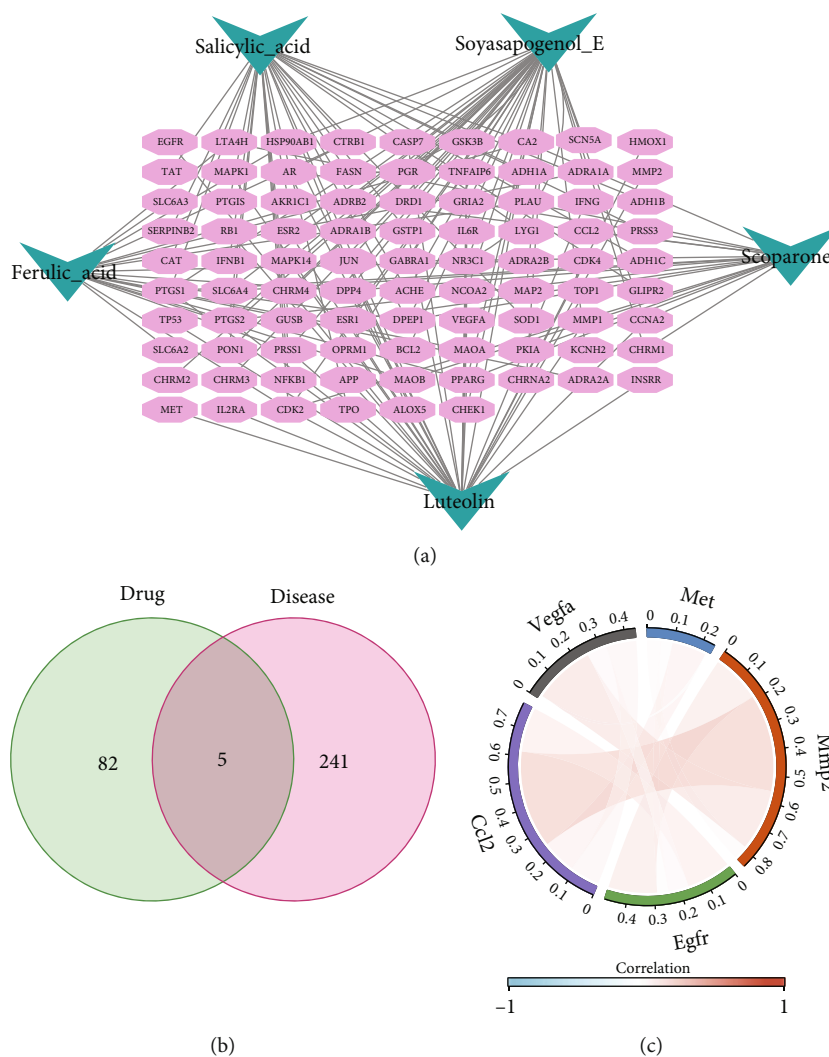


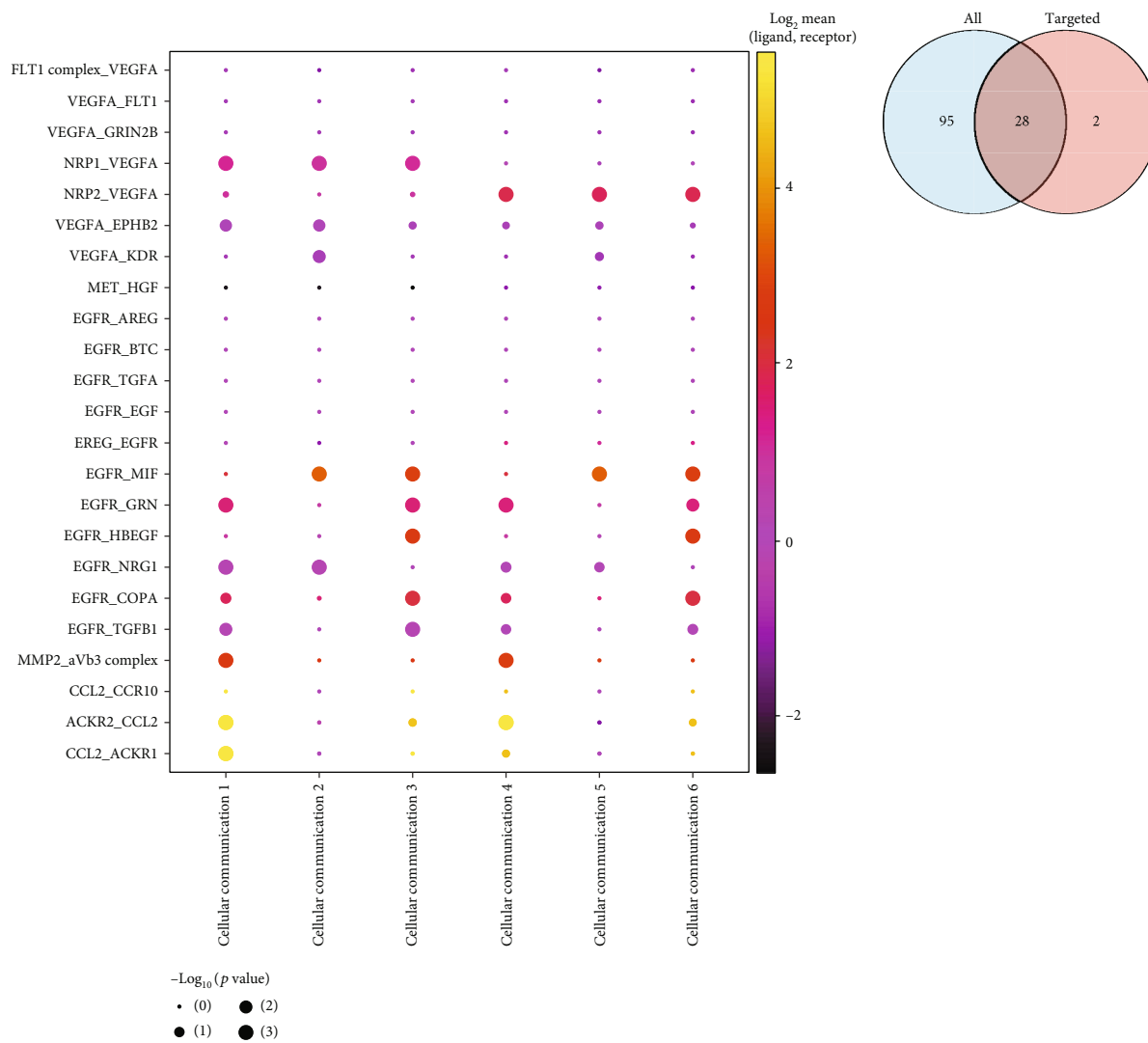
FIGURE 2: Potential role of *M. (L.) Pall.* (a) “drug-component-disease target genes” network; (b) drug target-MTJ ligand-receptor Venn diagram; (c) correlation analysis of five receptor-ligand-related genes (CCL2, EGFR, MMP2, MET, and VEGFA) demonstrated by the chord diagram.

2.3. Single-Cell Dataset-Based Receptor-Ligand Marker Analysis. Seurat results from our previous study of single-cell data analysis were used to perform ligand-receptor marker analysis [15]. Muscle-tendon junction (MTJ) cells were obtained from the GEO dataset of GSE168153 [14]. GSE168153 is a single-cell dataset describing fibroblasts in muscle tendon junctions. Receptor-ligand marker analysis of the MTJ cells was performed using the CellphoneDB algorithm (v2.1.2), to analyze the cellular interactions in MTJ regions [22]. After filtering with $P < 0.05$, key intercellular interactions were identified. The results were visualized using the dot_plot function in the CellphoneDB and the R software.

2.4. Screening and Molecular Docking Validation for the *M. (L.) Pall.* Cellular Action Targets in MTJs. R language and VennDiagram packages were used to obtain the *M. (L.) Pall.* targets on the MTJ cells [23]. The active ingredients of the drug were pretreated as shown in the following: screening of key targets and active ingredients in “drug-component-

target,” downloading 3D structures of active ingredients (mol2 format) from PubChem database, hydrogenation, charge addition, root detection of ligands, search and definition of rotatable bonds, etc. [24]. The 3D structure of the target protein was downloaded from the Protein Data Bank, all hydrogen atoms were added, Gasteiger charges were calculated, and nonpolar hydrogens were combined and saved in the pdbqt format using the AutoDock software [25]. The parameter exhaustiveness was set to 20, and other parameters were set to default values. AutoDock Vina 1.1.2 was used for molecular docking, and PyMOL was used for plotting [26].

2.5. Molecular Dynamics Simulation. To perform molecular dynamics simulations (MD), the force field parameters of luteolin were generated in this study using ACPYPE Server, an online tool [25, 27, 28]. Protein force fields are described by CHARMM [29]. TIP3P is for water modeling. The simulation was performed after a slow increase in system temperature from 0 K to 307 K. MD simulations were performed



(a)

(b)

FIGURE 3: Continued.

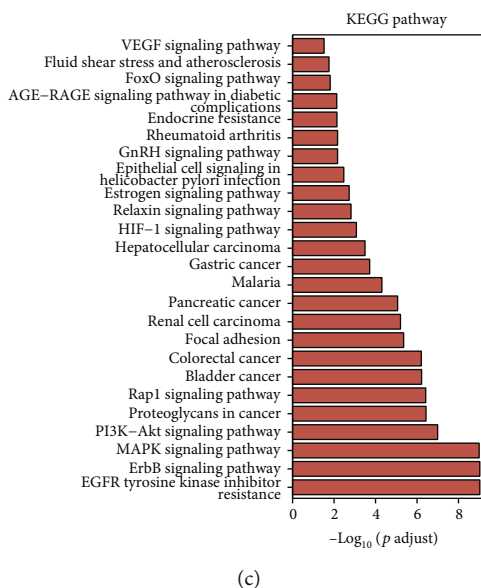


FIGURE 3: Ligand receptor analysis of MTJs targeted by *M. (L.) Pall.* (a) The key intercellular ligand-receptor interactions in MTJs, the vertical coordinate is the type of receptor-ligand linkage, and the horizontal coordinate is the corresponding cell-cell interaction; (b) “drug-component-disease target genes” network-MTJ ligand receptor-related pathway intersection analysis, “ALL” represents targets that *M. (L.) Pall.* may target, and “targeted” represents ligand-receptor-associated genes in (a); (c) enriched KEGG pathways.

using the GROMACS software under constant temperature and pressure conditions as shown in previous studies. Visualization of the results of molecular dynamics simulations was done using PyMOL [26, 29, 30].

2.6. Gene Ontology (GO) Functional Enrichment Analysis and Kyoto Encyclopedia of Genes and Genomes (KEGG) Pathway Enrichment Analysis. The study species was *homo sapiens*, and molecular function (MF), biological process (BP), and cellular component (CC) were used for GO enrichment analysis as previous researches [31–33]. The significance of the KEGG pathway was set at $P < 0.05$ to search for the major functional and in vivo pathways significantly enriched by the active ingredient targets. Bar graphs of the pathways in the GO and KEGG pathway enrichment analysis were plotted using the clusterProfiler toolkit in R and ggplot [19, 34].

2.7. Statistical Analysis. Statistical analyses were performed using the R software (version 3.6.3), and differences were significant at $P < 0.05$. Spearman’s method was used for correlation analysis, and the results of the analysis were presented as chord plots using the circlize package of the R software (version 0.4.12) [35].

3. Results

3.1. Screening for Potentially Active Compounds in *M. (L.) Pall.* Figure 1 depicts the research flow of this study. The active ingredients of *M. (L.) Pall.* are based on previous research results [16]. Six active ingredients were screened according to the following conditions: $OB \geq 30\%$ and $DL \geq 0.18$ (Table 1).

3.2. Potential *M. (L.) Pall.* Targets of on the MTJ Cells. Five of the six active ingredients had 87 corresponding targets (after excluding duplicates). The “herbal-active-component-disease target gene” regulatory network was constructed (Figure 2(a)). The red oval in the diagram represents the gene corresponding to the target protein. The green triangle represents the active ingredient. MTJ cells from the GSE168153 dataset were used for ligand-receptor analysis. All 246 potential ligand-receptor key genes were extracted. Cross-talk analysis revealed that *M. (L.) Pall.* might regulate the proteins of five genes (Figure 2(b)). Correlation analysis revealed that the expressions of CCL2, VEGFA, MET, MMP2, and EGFR were positively correlated with each other (Figure 2(c)).

3.3. Potential Effects of *M. (L.) Pall.* on MTJ Cells. As previously described, the data and cellular annotations for ligand-receptor maker analysis were obtained from GSE168153 database and our previous study, respectively. The receptor-ligand marker analysis of the MTJ cells was performed using the CellphoneDB algorithm (v2.1.2) (Figure 3(a)). The intersection analyses between the target enrichment pathways of *M. (L.) Pall.* and ligand receptor-related pathways of MTJs are shown in Figure 3(b). These target genes were found to be enriched in 28 KEGG pathways (EGFR tyrosine kinase inhibitor resistance, cancer-related pathway, epithelial cell signaling in *Helicobacter pylori* infection, rheumatoid arthritis, endocrine resistance; ErbB, MAPK, PI3K-Akt, Rap1, HIF-1, relaxin, estrogen, GnRH, and AGE-RAGE signaling pathways in diabetic complications; and so on). This suggests that *M. (L.) Pall.* may target some intercellular signaling pathways, such as neuropeptide-related, tumor-related, and stress direction-

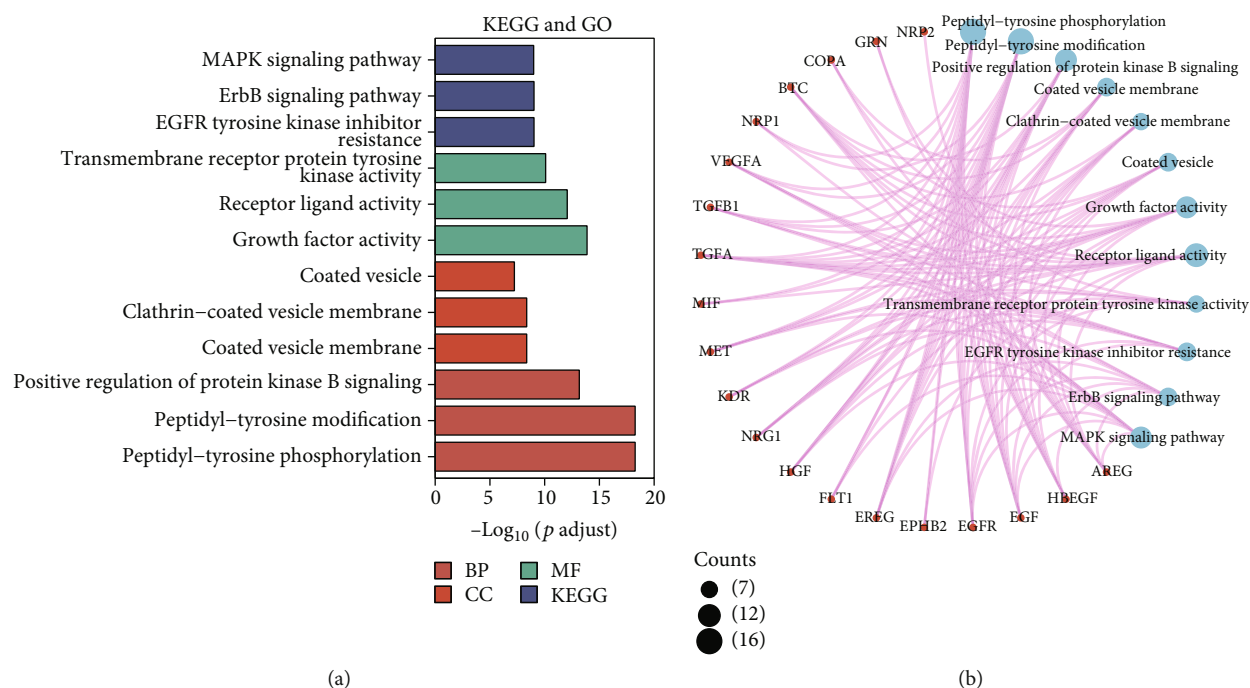


FIGURE 4: Enrichment analysis of core target proteins of *M. (L.) Pall.* (a) GO and KEGG enrichment analyses of core target proteins. (b) Distribution of the proteins in (a) from the GO and KEGG pathways.

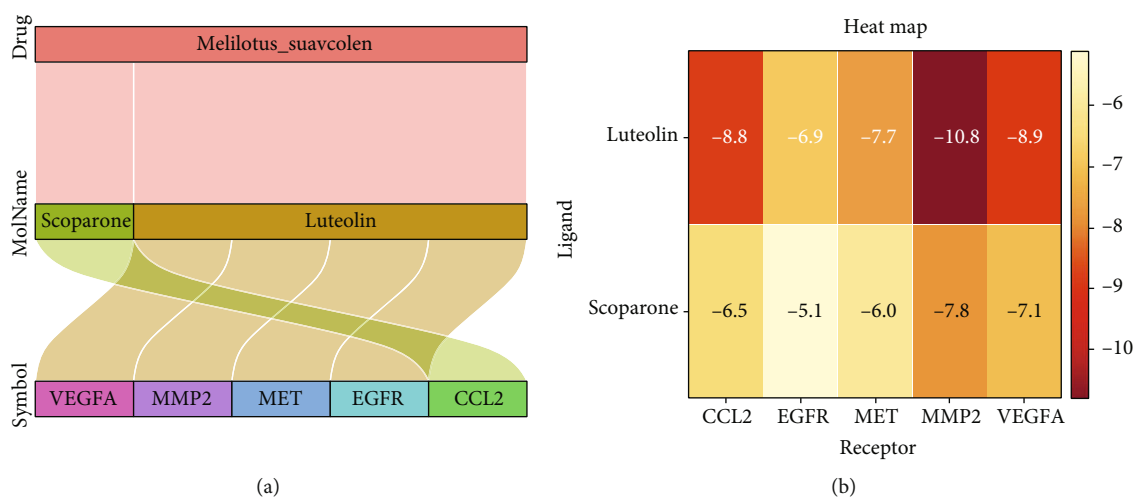


FIGURE 5: *M. (L.) Pall.* active ingredient-target protein regulatory relationships. (a) The Sankey diagram suggests that scoparone, the active ingredient of *M. (L.) Pall.* targets CCL2 and luteolin targets VEGFA, MMP2, MET, and EGFR. (b) Heat map showing the minimum binding energy of scoparone and luteolin to dock with target proteins CCL2, VEGFA, MMP2, MET, and EGFR.

related pathways (Figures 2(b) and 2(c)). These genes were also enriched in metabolic functions (MF), including transmembrane receptor protein tyrosine kinase, receptor-ligand, and growth factor activities. Moreover, these genes were found to be enriched in cellular functions (CC), including coated vesicle, clathrin-coated vesicle membrane, and coated vesicle membrane. In biological processes (BP), these genes are enriched in the positive regulation of protein kinase B signaling, peptidyl-tyrosine modification, and peptidyl-tyrosine phosphorylation (Figures 4(a) and 4(b)).

3.4. Regulatory Relationship and Molecular Docking Analysis of Active Ingredient-Target Proteins of *M. (L.) Pall.* Pharmacological database analysis suggests that scoparone, the active ingredient of *M. (L.) Pall.* targets CCL2 and luteolin targets VEGFA, MMP2, MET, and EGFR (Figure 5(a)). CCL2, VEGFA, MMP2, MET, and EGFR were molecularly docked to the two key pharmacodynamic components (scoparone, luteolin) of *M. (L.) Pall.* The lowest docking binding energy is shown in Figure 5(b). These molecular dockings are visualized in Figures 6(a)–6(e). The hydrogen bonds

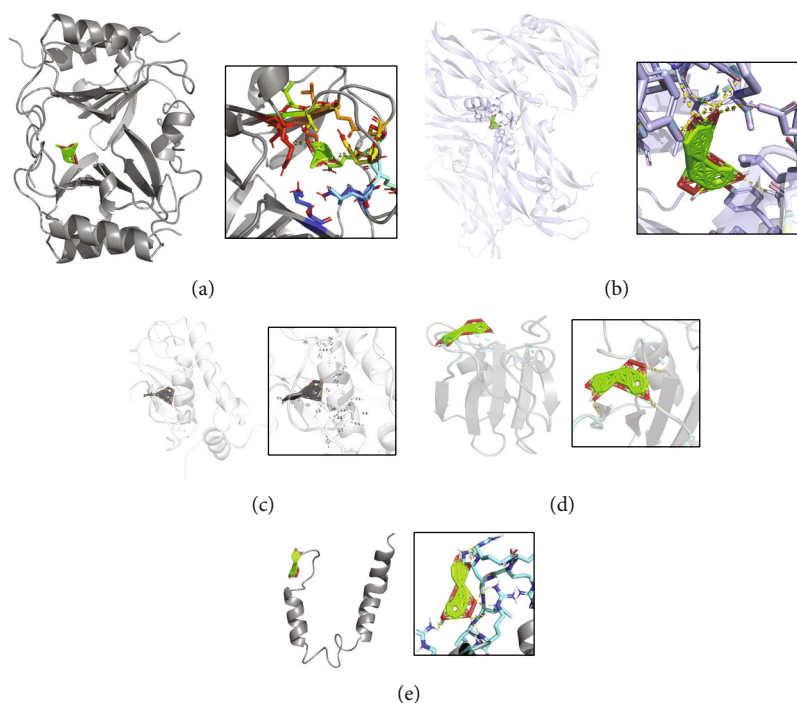


FIGURE 6: Schematic representation of molecular docking of target proteins with the active ingredients of *M. (L.) Pall.* (a) Interaction of scoparone with target CCL2 protein. (b) Interaction of luteolin with the target VEGFA protein. (c) Interaction of luteolin with the target MMP2 protein. (d) Interaction of luteolin with the target MET protein. (e) Interaction of luteolin with target EGFR protein. The dashed line indicates the hydrogen bond and marks the distance between the hydrogen bond and the compound.

are indicated using dashed lines, and the distances between the hydrogen bonds and the compounds are also marked. The scoparone target binding CCL2 protein has a free energy of -6.5 kJ/mol. The free energies of luteolin target binding energy for VEGFA, MMP2, MET, and EGFR proteins are -8.9 , -10.8 , -7.7 , and -6.9 kJ/mol, respectively. The minimum binding energies of these two key components to CCL2, VEGFA, MMP2, MET, and EGFR were less than -5.0 kJ/mol suggesting that *M. (L.) Pall.* exerts its effects mainly by targeting these components through scoparone and luteolin.

3.5. Molecular Dynamics Simulations of MMP2 and Luteolin.

In the above molecular docking analysis, MMP2 and luteolin had the minimum binding free energy. The free energy of luteolin target binding energy for MMP2 is -10.8 kJ/mol. To further assess the binding efficacy of MMP2 and luteolin, MD simulations were performed (Figure 7(a)). Due to the interaction between MMP2 and luteolin, the root mean square displacement (RMSD) was found to increase at first and then stabilise (Figure 7(b)). The radius of gyration (Rg) of the MMP2-luteolin complex was also found to stabilise with the time passing (Figure 7(c)). In addition, the number of hydrogen bonds formed by MMP2 with luteolin remained in a relatively stable range (Figure 7(d)). The overall free energy in the system was also found to be stable (Figure 7(e)). Finally, MD simulations revealed that luteolin can stably target binding to MMP2.

4. Discussion

To the best of our knowledge, this study is the first to assess the impact of *M. (L.) Pall.* on the musculotendinous junction. According to the TCMSP database, *M. (L.) Pall.* has five active ingredients ($OB \geq 30\%$ and $DL \geq 0.18$) potentially acting on 87 targets. Therefore, the “herb-active ingredient-disease target gene” network was constructed. We found that *M. (L.) Pall.* influences the interaction of fibroblasts in musculotendon junctions and affects muscle repair patterns through the modulation of five ligand receptor-related proteins (CCL2, VEGFA, MMP2, MET, and EGFR) using the active ingredients luteolin and scoparone. And MD simulations revealed that luteolin can stably target binding to MMP2.

Scoparone is a naturally occurring coumarin found in green plants. It is purified from a lipid-lowering herb that reduces the proliferation of human peripheral blood mononuclear cells, scavenges reactive oxygen species, inhibits tyrosine kinase, and enhances the production of prostaglandins [36]. Recent studies have confirmed that scoparone has various biological activities such as antifibrosis, antioxidant, and fat differentiation inhibition [37–39]. Scoparone was also found to inhibit high-glucose-induced activation of the ERK1/2 signaling pathway in thylakoid cells and played an active role in inhibiting the accumulation of extracellular matrix in the high-glucose microenvironment [40]. In this study, scoparone was found to target CCL2. CCL2 is a ligand for CCR2. Inhibition of CCR2 after injury promotes skeletal muscle

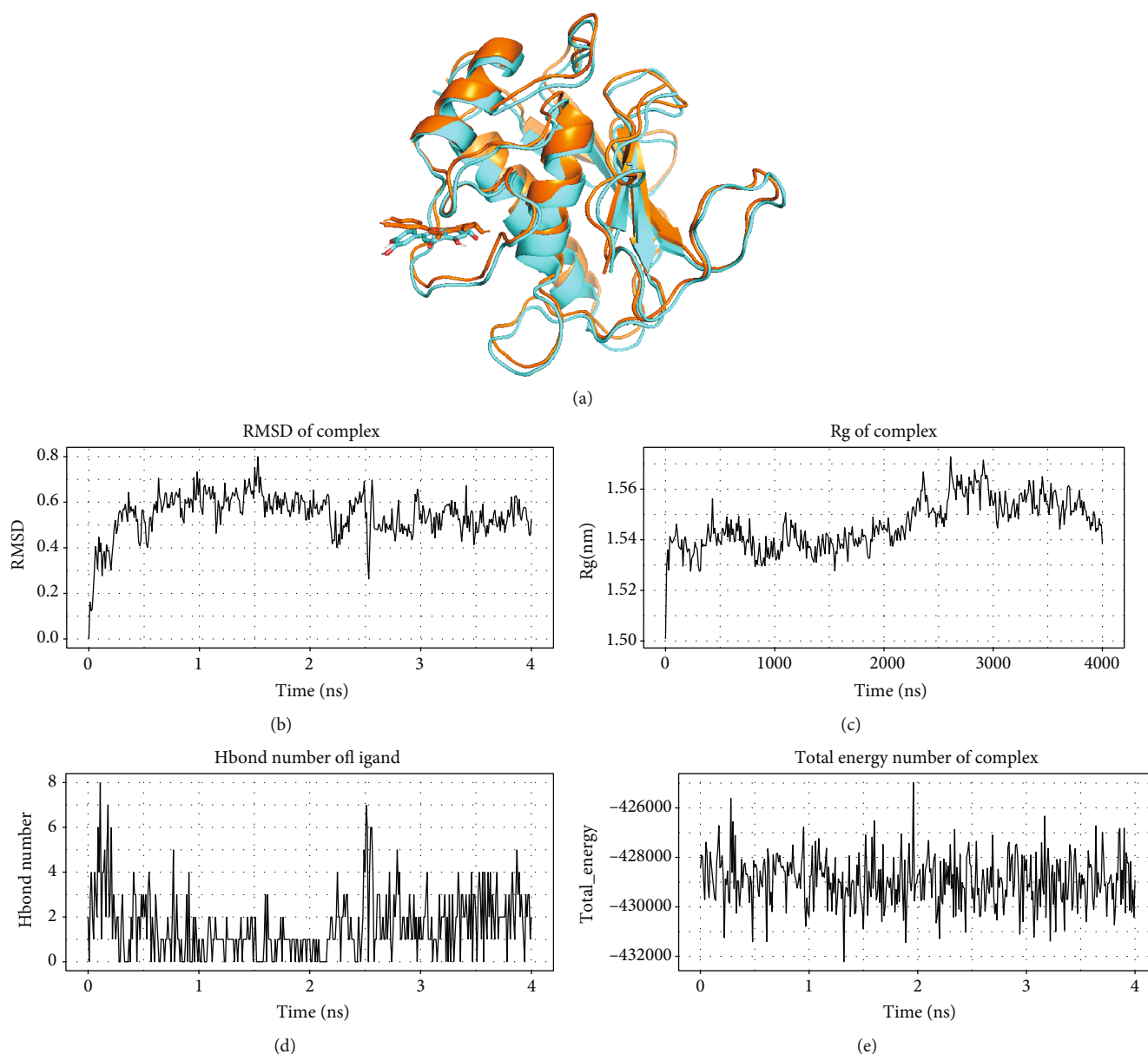


FIGURE 7: Molecular dynamics simulations of MMP2 and luteolin. (a) Conformational changes of the complex before and after MD, brown indicates before MD, and blue indicates after MD. (b) Variation of the root mean square displacement (RMSD) of the MMP2-luteolin complex. (c) Variation of the radius of gyration (Rg) of the MMP2-luteolin complex with time. (d) Variation of the number of hydrogen bonds formed between MMP2 and luteolin with time. (e) The free energy of binding between the small molecule ligand and the protein over time.

regeneration and function recovery [41, 42]. Our study suggests that scoparone may inhibit the function of CCR2 by binding to CCL2, and this may be a potential mechanism for M. (L.) Pall. to promote skeletal muscle regeneration.

Recent studies have found that luteolin protects skeletal muscles from attrition caused by inflammation and downregulates the expression of proteins associated with muscle catabolism [43]. Luteolin increased muscle strength in fatigued subjects and improved skeletal muscle contraction during ischemia and reperfusion [44]. In this study, luteolin targeted VEGFA, MMP2, MET, and EGFR. Luteolin inhibits VEGFA and affects microvascular networks formed during

neovascularization in mice [45]. In tumors, luteolin inhibits MMP2 and MET [46–48]. Luteolin also inhibits downstream signaling molecules activated by EGFR, especially the Akt and MAPK signaling pathways [49].

Luteolin was found to target MMP2 in MD simulations. Elevated levels of MMP2 expression are associated with insulin resistance due to extracellular matrix (ECM) remodelling in skeletal muscle [50]. This suggests that luteolin targeting of MMP2 may have the potential to improve insulin resistance due to ECM. MMP2 has been found to be widespread in skeletal muscle, and therefore, the study of its function is important for exploring the repair of skeletal muscle after injury

[51]. For example, both exogenous hydrogen sulphide and electroacupuncture treatments can improve skeletal muscle injury and reduce skeletal muscle fibrosis by downregulating MMP2 and related pathways [5, 52]. In the present study, luteolin was found to target MMP2, which may contribute to skeletal muscle injury repair.

This study provides new data supporting the treatment of sports injuries using M. (L.) Pall. and provides a theoretical basis for clinical application. All the core components of M. (L.) Pall. were screened and docked successfully with their key targets. The core components of M. (L.) Pall. have good binding activities to their key targets, suggesting that they can effectively treat skeletal muscles. However, more Chinese medicine databases need to be used, and target prediction databases need to be improved. This study did not directly examine the chronic muscle injury dataset, but rather by examining the MTJ fibroblastic dataset, which may be biased. Furthermore, more in vivo and ex vivo clinical studies are also needed to validate the mechanisms of action M. (L.) Pall. in the treatment of chronic skeletal muscle injury.

5. Conclusion

In summary, this study demonstrates that M. (L.) Pall. can skeletal muscle injury by acting on CCL2, VEGFA, MMP2, MET, and EGFR, through luteolin and scoparone. They are the key active ingredients of M. (L.) Pall. and affect intercellular signaling, such as neuropeptide-related, tumor-related, and stress-related pathways. M. (L.) Pall. may influence the interaction of fibroblasts in muscle tendon junctions to affect muscle repair patterns. Molecular docking analysis validated some of the network pharmacology results and confirmed the multicomponent, multitarget, and multipathway characteristics of M. (L.) Pall. in the treatment of skeletal muscle injury.

Data Availability

Muscle tendon junction (MTJs) cells are from the GEO dataset in the GSE168153 database.

Conflicts of Interest

The authors declare that they have no conflicts of interest.

Authors' Contributions

Yisheng Chen, Zhiwen Luo, Jinrong Lin, and Beijie Qi contributed equally to this work.

Acknowledgments

Thanks are due to all those who worked on this study. This study was supported by grants from the National Natural Science Foundation of China (Nos. 82102634, 81972062, and 81772419) and the Medical and Health Science and Technology Development Project of Shandong Province (2018WS147). This work was also supported by the Project of the Key Clinical Medicine Center of Shanghai (No. 2017ZZ01006), the Sanming Project of Medicine in Shenzhen (No. SZSM201612078), the Development Project

of Shanghai Peak Disciplines-Integrative Medicine (No. 20180101), and the Shanghai Committee of Science and Technology (No. 19441901600). We thank Bullet Edits Limited for the linguistic editing and proofreading of the manuscript.

References

- [1] M. Ilhan, Z. Ali, I. A. Khan, H. Taştan, and E. Küpeli Akkol, "The regression of endometriosis with glycosylated flavonoids isolated from *Melilotus officinalis* (L.) Pall. in an endometriosis rat model," *Taiwanese Journal of Obstetrics & Gynecology*, vol. 59, no. 2, pp. 211–219, 2020.
- [2] G. Paun, E. Neagu, C. Albu, S. Savin, and G. L. Radu, "In vitro evaluation of antidiabetic and anti-inflammatory activities of polyphenolic-rich extracts from *Anchusa officinalis* and *Melilotus officinalis*," *ACS Omega*, vol. 5, no. 22, pp. 13014–13022, 2020.
- [3] I. W. Southon, J. Buckingham, F. A. Bisby, and J. B. Harborne, *Phytochemical Dictionary of the Leguminosae*, Chapman and Hall/CRC, 1994.
- [4] China Ministry of Health, *People's Republic of China Ministry of Health Drug Standard Tibetan Medicine. Volume 1. in 65*, Chemical Industry Press, 1995.
- [5] H. Han, M. Li, H. Liu, and H. Li, "Electroacupuncture regulates inflammation, collagen deposition and macrophage function in skeletal muscle through the TGF- β 1/Smad3/p38/ERK1/2 pathway," *Experimental and Therapeutic Medicine*, vol. 22, no. 6, p. 1457, 2021.
- [6] T. A. H. Järvinen, T. L. N. Järvinen, M. Kääriäinen et al., "Muscle injuries: optimising recovery," *Best Practice & Research. Clinical Rheumatology*, vol. 21, no. 2, pp. 317–331, 2007.
- [7] Y. Chen, Y. X. Cai, X. R. Kang et al., "Predicting the risk of sarcopenia in elderly patients with patellar fracture: development and assessment of a new predictive nomogram," *PeerJ*, vol. 8, article e8793, 2020.
- [8] M. L. Bayer, M. Hoegberget-Kalisz, R. B. Svensson et al., "Chronic sequelae after muscle strain injuries: influence of heavy resistance training on functional and structural characteristics in a randomized controlled trial," *The American Journal of Sports Medicine*, vol. 49, no. 10, pp. 2783–2794, 2021.
- [9] S. Mannava, J. F. Plate, P. W. Whitlock et al., "Evaluation of in vivo rotator cuff muscle function after acute and chronic detachment of the supraspinatus tendon: an experimental study in an animal model," *Journal of Bone and Joint Surgery*, vol. 93, no. 18, pp. 1702–1711, 2011.
- [10] S. Corti, S. Strazzer, R. del Bo et al., "A subpopulation of murine bone marrow cells fully differentiates along the myogenic pathway and participates in muscle repair in the mdx dystrophic mouse," *Experimental Cell Research*, vol. 277, no. 1, pp. 74–85, 2002.
- [11] Z. Luo, Y. Sun, B. Qi et al., "Human bone marrow mesenchymal stem cell-derived extracellular vesicles inhibit shoulder stiffness via let-7a/Tgfb1 axis," *Bioactive Materials*, vol. 17, pp. 344–359, 2022.
- [12] A. L. Mackey and M. Kjaer, "Connective tissue regeneration in skeletal muscle after eccentric contraction-induced injury," *Journal of Applied Physiology*, vol. 122, no. 3, pp. 533–540, 2017.
- [13] X. Yin, T. Yu, B. Chen et al., "Spatial distribution of motor endplates and its adaptive change in skeletal muscle," *Theranostics*, vol. 9, no. 3, pp. 734–746, 2019.

- [14] J. Esteves de Lima, C. Blavet, M. A. Bonnin et al., “Unexpected contribution of fibroblasts to muscle lineage as a mechanism for limb muscle patterning,” *Nature Communications*, vol. 12, no. 1, p. 3851, 2021.
- [15] Y. Chen, C. Chen, X. Xiao, Z. Huang, X. Huang, and W. Yao, “TNF- α induces neutrophil apoptosis delay and promotes intestinal ischemia-reperfusion-induced lung injury through activating JNK/FoxO3a pathway,” *Oxidative Medicine and Cellular Longevity*, vol. 2021, 13 pages, 2021.
- [16] Y.-T. Liu, P. H. Gong, F. Q. Xiao et al., “Chemical constituents and antioxidant, anti-inflammatory and anti-tumor activities of *Melilotus officinalis* (Linn.) Pall,” *Molecules*, vol. 23, no. 2, p. 271, 2018.
- [17] M. Shahrousvand, V. Haddadi-Asl, and M. Shahrousvand, “Step-by-step design of poly (ϵ -caprolactone) /chitosan/*Melilotus officinalis* extract electrospun nanofibers for wound dressing applications,” *International Journal of Biological Macromolecules*, vol. 180, pp. 36–50, 2021.
- [18] P. De Benedetti and F. Fanelli, “Ligand-receptor communication and drug design,” vol. 10, no. 2, pp. 186–193, 2009.
- [19] J. W. Peng, “Communication breakdown: protein dynamics and drug design,” *Structure*, vol. 17, no. 3, pp. 319–320, 2009.
- [20] J. Ru, P. Li, J. Wang et al., “TCMSP: a database of systems pharmacology for drug discovery from herbal medicines,” *Journal of Cheminformatics*, vol. 6, no. 1, p. 13, 2014.
- [21] P. Shannon, A. Markiel, O. Ozier et al., “Cytoscape: a software environment for integrated models of biomolecular interaction networks,” *Genome Research*, vol. 13, no. 11, pp. 2498–2504, 2003.
- [22] M. Efremova, M. Vento-Tormo, S. A. Teichmann, and R. Vento-Tormo, “CellPhoneDB: inferring cell-cell communication from combined expression of multi-subunit ligand-receptor complexes,” *Nature Protocols*, vol. 15, no. 4, pp. 1484–1506, 2020.
- [23] H. Chen and P. C. Boutros, “VennDiagram: a package for the generation of highly-customizable Venn and Euler diagrams in R,” *BMC Bioinformatics*, vol. 12, no. 1, p. 35, 2011.
- [24] S. Kim, “Getting the most out of PubChem for virtual screening,” *Expert Opinion on Drug Discovery*, vol. 11, no. 9, pp. 843–855, 2016.
- [25] O. Trott and A. J. Olson, “AutoDock Vina: improving the speed and accuracy of docking with a new scoring function, efficient optimization, and multithreading,” *Journal of Computational Chemistry*, vol. 31, no. 2, pp. NA–461, 2009.
- [26] D. Seeliger and B. L. de Groot, “Ligand docking and binding site analysis with PyMOL and AutoDock/Vina,” *Journal of Computer-Aided Molecular Design*, vol. 24, no. 5, pp. 417–422, 2010.
- [27] S. Kim, A. Gindulyte, J. Zhang, P. A. Thiessen, and E. E. Bolton, “PubChem periodic table and element pages: improving access to information on chemical elements from authoritative sources,” *Chemistry Teacher International*, vol. 3, no. 1, pp. 57–65, 2021.
- [28] A. W. Sousa da Silva and W. F. Vranken, “ACYPPE - Ante-Chamber Python Parser interface,” *BMC Research Notes*, vol. 5, no. 1, p. 367, 2012.
- [29] M. J. Abraham, T. Murtola, R. Schulz et al., “GROMACS: high performance molecular simulations through multi-level parallelism from laptops to supercomputers,” *SoftwareX*, vol. 1–2, pp. 19–25, 2015.
- [30] Y. Zhang, J. Zhang, C. Sun, and F. Wu, “Identification of the occurrence and potential mechanisms of heterotopic ossification associated with 17-beta-estradiol targeting MKX by bioinformatics analysis and cellular experiments,” *PeerJ*, vol. 9, article e12696, 2022.
- [31] Y. Chen, X. R. Kang, Z. H. Zhou et al., “MiR-1908/EXO1 and MiR-203a/FOS, regulated by *scd1*, are associated with fracture risk and bone health in postmenopausal diabetic women,” *Aging*, vol. 12, no. 10, pp. 9549–9584, 2020.
- [32] W.-W. Lin, L.-T. Xu, Y.-S. Chen, K. Go, C. Sun, and Y.-J. Zhu, “Single-cell transcriptomics-based study of transcriptional regulatory features in the mouse brain vasculature,” *BioMed Research International*, vol. 2021, Article ID 7643209, 15 pages, 2021.
- [33] J. Wu, J. Qin, L. Li et al., “Roles of the immune/methylation/autophagy landscape on single-cell genotypes and stroke risk in breast cancer microenvironment,” *Oxidative Medicine and Cellular Longevity*, vol. 2021, Article ID 5633514, 32 pages, 2021.
- [34] G. Yu, L.-G. Wang, Y. Han, and Q.-Y. He, “clusterProfiler: an R package for comparing biological themes among gene clusters,” *Integrative Biology*, vol. 16, no. 5, pp. 284–287, 2012.
- [35] Z. Gu, L. Gu, R. Eils, M. Schlesner, and B. Brors, “Circize implements and enhances circular visualization in R,” *Bioinformatics*, vol. 30, no. 19, pp. 2811–2812, 2014.
- [36] J. R. Hoult and M. Payá, “Pharmacological and biochemical actions of simple coumarins: natural products with therapeutic potential,” *General Pharmacology*, vol. 27, no. 4, pp. 713–722, 1996.
- [37] B. Fu, Y. Su, X. Ma, C. Mu, and F. Yu, “Scoparone attenuates angiotensin II-induced extracellular matrix remodeling in cardiac fibroblasts,” *Journal of Pharmacological Sciences*, vol. 137, no. 2, pp. 110–115, 2018.
- [38] J.-R. Noh, Y. H. Kim, J. H. Hwang et al., “Scoparone inhibits adipocyte differentiation through down-regulation of peroxisome proliferators-activated receptor γ in 3T3-L1 preadipocytes,” *Food Chemistry*, vol. 141, no. 2, pp. 723–730, 2013.
- [39] L. Lyu, J. Chen, W. Wang et al., “Scoparone alleviates Ang II-induced pathological myocardial hypertrophy in mice by inhibiting oxidative stress,” *Journal of Cellular and Molecular Medicine*, vol. 25, no. 6, pp. 3136–3148, 2021.
- [40] Y. Wang, M. Wang, B. Chen, and J. Shi, “Scoparone attenuates high glucose-induced extracellular matrix accumulation in rat mesangial cells,” *European Journal of Pharmacology*, vol. 815, pp. 376–380, 2017.
- [41] R. S. Blanc, J. G. Kallenbach, J. F. Bachman, A. Mitchell, N. D. Paris, and J. V. Chakkalakal, “Inhibition of inflammatory CCR2 signaling promotes aged muscle regeneration and strength recovery after injury,” *Nature Communications*, vol. 11, no. 1, p. 4167, 2020.
- [42] J. G. Tidball, “Inflammatory processes in muscle injury and repair,” *American Journal of Physiology. Regulatory, Integrative and Comparative Physiology*, vol. 288, no. 2, pp. R345–R353, 2005.
- [43] T. Chen, B. Li, Y. Xu, S. Meng, Y. Wang, and Y. Jiang, “Luteolin reduces cancer-induced skeletal and cardiac muscle atrophy in a Lewis lung cancer mouse model,” *Oncology Reports*, vol. 40, no. 2, pp. 1129–1137, 2018.
- [44] M. Gelabert-Rebato, J. C. Wiebe, M. Martin-Rincon et al., “*Mangifera indica* L. leaf extract in combination with luteolin or quercetin enhances VO₂peak and peak power output, and preserves skeletal muscle function during ischemia-reperfusion in humans,” *Frontiers in Physiology*, vol. 9, p. 740, 2018.

- [45] Y. Dai, H. Zheng, Z. Liu, Y. Wang, and W. Hu, "The flavonoid luteolin suppresses infantile hemangioma by targeting FZD6 in the Wnt pathway," *Investigational New Drugs*, vol. 39, no. 3, pp. 775–784, 2021.
- [46] H. Liu, Z. Zeng, S. Wang et al., "Main components of pomegranate, ellagic acid and luteolin, inhibit metastasis of ovarian cancer by down-regulating MMP2 and MMP9," *Cancer Biology & Therapy*, vol. 18, no. 12, pp. 990–999, 2017.
- [47] X. Yao, W. Jiang, D. Yu, and Z. Yan, "Luteolin inhibits proliferation and induces apoptosis of human melanoma cells in vivo and in vitro by suppressing MMP-2 and MMP-9 through the PI3K/AKT pathway," *Food & Function*, vol. 10, no. 2, pp. 703–712, 2019.
- [48] W. Masraksa, S. Tanasawet, P. Hutamekalin, T. Wongtawatchai, and W. Sukketsiri, "Luteolin attenuates migration and invasion of lung cancer cells via suppressing focal adhesion kinase and non-receptor tyrosine kinase signaling pathway," *Nutrition Research and Practice*, vol. 14, no. 2, pp. 127–133, 2020.
- [49] D. M. Anson, R. M. Wilcox, E. D. Huseman et al., "Luteolin decreases epidermal growth factor receptor-mediated cell proliferation and induces apoptosis in glioblastoma cell lines," *Basic & Clinical Pharmacology & Toxicology*, vol. 123, no. 6, pp. 678–686, 2018.
- [50] C. S. Tam, R. Chaudhuri, A. T. Hutchison, D. Samocha-Bonet, and L. K. Heilbronn, "Skeletal muscle extracellular matrix remodeling after short-term overfeeding in healthy humans," *Metabolism*, vol. 67, pp. 26–30, 2017.
- [51] X. Ren, G. D. Lamb, and R. M. Murphy, "Distribution and activation of matrix metalloproteinase-2 in skeletal muscle fibers," *American Journal of Physiology-Cell Physiology*, vol. 317, no. 3, pp. C613–C625, 2019.
- [52] L. Zhao, X. Liu, J. Zhang, G. Dong, W. Xiao, and X. Xu, "Hydrogen sulfide alleviates skeletal muscle fibrosis via attenuating inflammation and oxidative stress," *Frontiers in Physiology*, vol. 11, article 533690, 2020.